Atmos. Chem. Phys. Discuss., 14, 14159–14199, 2014
www.atmos-chem-phys-discuss.net/14/14159/2014/
doi:10.5194/acpd-14-14159-2014

Atmospheric Chemistry and Physics
Discussions
Open Access

Submicron aerosol source apportionment of wintertime pollution in Paris, France by Double Positive Matrix Factorization (PMF^2) using Aerosol Chemical Speciation Monitor (ACSM) and multi-wavelength Aethalometer

J.-E. Petit[1,2], O. Favez[1], J. Sciare[2], F. Canonaco[3], P. Croteau[4], G. Močnik[5], J. Jayne[4], D. Worsnop[4], and E. Leoz-Garziandia[1]

[1]Institut National de l'Environnement Industriel et des RISques, INERIS, Parc Technologique ALATA BP2, 60550 Verneuil-en-Halatte, France
[2]Laboratoire des Sciences du Climat et de l'Environnement, LSCE, UMR8212, CNRS-CEA-UVSQ, 91191 Gif-sur-Yvette, France
[3]Laboratory of Atmospheric Chemistry, Paul Scherrer Institute, 5232 PSI Villigen, Switzerland
[4]Aerodyne Research, Inc. 45 Manning Road Billerica, MA, USA
[5]Aerosol d.o.o., Kamniška 41, 1000 Ljubljana, Slovenia

Received: 6 April 2014 – Accepted: 15 May 2014 – Published: 2 June 2014

Correspondence to: J.-E. Petit (jean-eudes.petit-etudiant@ineris.fr)

Published by Copernicus Publications on behalf of the European Geosciences Union.

Abstract

Online non-refractory submicron Aerosol Mass Spectrometer (AMS) measurements in urban areas have successfully allowed the apportionment of specific sources and/or physical and chemical properties of the organic fraction. However, in order to be fully representative of PM pollution, a comprehensive source apportionment analysis is needed by taking into account all major components of submicron aerosols, creating strengthened bonds between the organic components and pollution sources. We present here a novel two-step methodology to perform such an analysis, by taking advantage of high time resolution of monitoring instruments: the Aerosol Chemical Speciation Monitor (ACSM) and the multi-wavelength absorption measurements (Aethalometer AE31) in Paris, France. As a first step, organic aerosols (OA) were deconvoluted to hydrocarbon-like OA (HOA), Biomass Burning OA (BBOA) and Oxygenated OA (OOA) with Positive Matrix Factorization, and black carbon was deconvolved into its wood burning and fossil fuel combustion fractions. A second PMF analysis was then carried out with organic factors, BC fractions and inorganic species (nitrate, sulfate, ammonium, chloride), leading to a four-factor solution allowing real-time characterization of the major sources of PM_1. Outputs of this PMF^2 include two dominant combustion sources (wood burning and traffic) as well as semi-volatile and low-volatile secondary aerosols. While HOA is found to be emitted by both wood burning and traffic, the latter sources occurred to significantly contribute also to OOA.

1 Introduction

The source apportionment of aerosolized particulate matter has become one of the main concerns of air quality studies as well as stakeholder initiatives. This is primarily related to growing evidence of their adverse health effects (Pope and Dockery, 2006; Pope et al., 2004), impacts on air quality, by means of frequent exceedances of EU limit values at urban sites, and, globally, climate change, through its direct and indirect

Title Page
Abstract | Introduction
Conclusions | References
Tables | Figures
◀| |▶
◀ ▶
Back | Close
Full Screen / Esc
Printer-friendly Version
Interactive Discussion

effects on the Earth's radiative balance (Haywood and Boucher, 2000; Rosenfeld et al., 2008). Moreover, despite geographical disparities, the understanding of the particulate matter in urban areas remains complex by virtue of its chemical composition and the multitude of emission sources.

The organic aerosol (OA) fraction gathers in itself all of the aforementioned challenges. It is especially complex and dynamic, exhibiting an outstanding number of molecules, structures, transformation pathways, and physical and chemical properties. While primary OA are linked to local/regional emission sources (e.g. traffic and biomass burning), secondary OA usually result from the chemical transformation of pre-existing particles or from the condensation of gaseous precursors through several oxidation reactions, and thus present diverse degrees of oxidation. This issue is emphasized by strong discrepancies between laboratory and ambient measurements, and traditional SOA formation models, which could underestimate secondary particle formation and/or the condensation of Oxidized Primary Organic Aerosols (OPOA) (Robinson et al., 2007), especially for wood burning (Adler et al., 2011; Grieshop et al., 2009; Heringa et al., 2011; Robinson et al., 2006) and traffic (Chirico et al., 2010; Platt et al., 2013; Sage et al., 2008; Weitkamp et al., 2007) emissions.

Previous worldwide high-time resolution measurements of the chemical composition of non-refractory submicron aerosols (nitrate, sulfate, ammonium, chloride and organic matter), performed by Aerosol Mass Spectrometers (Aerodyne Research, Inc., ARI), highlight the quantitative predominance of OA, and have enhanced the understanding of the chemical and physical transformations of OA (Jimenez et al., 2009). The Aerosol Chemical Speciation Monitor (ACSM, ARI) shares the same technology and measurement principle as the regular AMS, except for size distribution information, and allows for robust long term ambient monitoring (Ng et al., 2010). Through the use of source-receptor model toolkits based on Positive Matrix Factorization (PMF; Ulbrich et al., 2009; Canonaco et al., 2013), both instruments allow for the deconvolution of OA into several subgroups characterized by their fragmentation fingerprints. Such source apportionment (SA) studies are nowadays widely reported in the literature (e.g. Lanz et al., 2010; Zhang et al., 2011; Crippa et al., 2013a) and have led to a significant improvement of our understanding of OA sources and atmospheric ageing. This type of statistical analysis commonly leads to the identification of several organic factors presenting various degrees of oxidation and/or having mass spectra signatures which can be related to specific tracers of a given emission source. Oxidized Organic Aerosol (OOA) are thought to be linked to Secondary Organic Aerosols (SOA) which can be further divided into semi-volatile and low-volatile fractions (SV-OOA and LV-OOA, respectively); while Hydrogenated Organic Aerosols (HOA) are usually considered as Primary Organic Aerosols (POA) emitted by combustion of fossil fuels (gasoline, diesel or crude oil for instance). Other OA sources such as Biomass Burning Organic Aerosols (BBOA) or Cooking Organic Aerosols (COA) were also observed depending on the site location and the season of study (Lanz et al., 2007; Allan et al., 2010; Crippa et al., 2013b, c).

However, OA source apportionment does not address the mass of the contributions from different pollution sources, as other carbonaceous (e.g. Black Carbon) and inorganic species (nitrate, sulfate and ammonium) account for a significant fraction of PM_1 mass. Since the AMS also allows for the measurement of non-refractory inorganic compounds, some alternative and innovative approaches recently make use of PMF analyses including the latter species. For instance, Sun et al. (2012) proposed the combination of organic MS and specific inorganic fragments to investigate the links between these two fractions. More recently, McGuire et al. (2014) used the total AMS mass spectra to simultaneously take organic and inorganic fragments into account. These novel methodologies are of prime interest for an improved understanding of pollution sources and their evolution in the atmosphere. The combination of measurements obtained from different instruments is also quite helpful. In this context, Crippa et al. (2013b) combined organic AMS data with PTR-MS data, creating strengthened bonds between particulate phase organics and their gaseous precursors. Including tracer measurements of other individual species, molecules, or elements (e.g. BC fractions, levoglucosan, transition metals) may also greatly improve PM_1 source apportionments. On-line measurements of specific organic tracers and transition metals might be envisaged for networking activities in near future. For BC, among the various instruments that already allow its monitoring in ambient air, the multi-wavelength Aethalometer (Magee Scientific) offers the possibility for absorption spectral dependence analyses of the various absorbing materials (e.g. fossil fuel BC and wood burning BC, as defined by Sandradewi et al., 2008 and Favez et al., 2010).

Here, we propose a novel methodology using conventional AMS/PMF approaches and external datasets. This methodology shares the same goal than innovative approaches mentioned above, but has been developed with ACSM measurements, which shows less sensitivity than High Resolution AMS measurements. The first step of the presented work aims to identify and characterize wintertime OA sources and transformation processes in the region of Paris, as usually performed with mass spectrometer datasets for about 10 years. Then, going beyond a single OA source apportionment, the resulted organic tracers combined with inorganic species (nitrate, sulfate, ammonium and chloride) and source specific black carbon concentrations, are used for PM_1 source apportionment.

2 Methodology

2.1 Measurement site and instrumentation

Measurements were conducted at the SIRTA atmospheric supersite (Site Instrumental de Recherche par Télédétection Atmosphérique, 2.15° E; 48.71° N; 150 m a.s.l.; Haeffelin et al., 2005; http://sirta.ipsl.fr). This site is located about twenty kilometers southwest of Paris and is representative of suburban background conditions of the Ile-de-France region (Sciare et al., 2011; Crippa et al., 2013b; Freutel et al., 2013). Data presented here are part of the long-term in-situ aerosol properties monitoring observations performed from mid-2011 onwards at SIRTA within the EU-FP7 (European Union Seventh Framework Programme for Research) ACTRIS program (Aerosols, Clouds, and Trace gases Research InfraStructure Network; http://www.actris.net). We selected the period from 31 January to 26 March 2012 for its representativeness of late winter–early spring conditions, a period of the year with frequent exceedances of the European daily PM_{10} threshold ($50\,\mu g\,m^{-3}$) and a significant contribution towards exceeding the annual mean $PM_{2.5}$ target value ($20\,\mu g\,m^{-3}$). The combination of enhanced domestic heating emissions and stagnant atmospheric conditions in late winter–early spring is propitious for the accumulation of pollutants within the boundary layer, and for photochemical processes influencing air quality (Favez et al., 2012; Waked et al., 2014; Bressi et al., 2013). An overview of meteorological parameters and submicron aerosol chemical composition during the selected period is shown in Fig. 1, illustrating the occurrence of high concentrations of organics initially and ammonium nitrate later in the measurement period.

Since summer 2011, measurements of the chemical composition of non-refractory submicron aerosol have been carried out using an ACSM. This recent instrument shares the same general structure with the AMS but has been specifically developed for long-term monitoring. An exhaustive description of this instrument is available in Ng et al. (2011). Briefly, submicron particles are sampled at $3\,L\,min^{-1}$ with a $PM_{2.5}$ cut-off, and sub-sampled at $85\,mL\,min^{-1}$ through an aerodynamic focusing lens toward a conical porous tungsten vaporizer heated to 600 °C. Non-refractory submicron particles are then flash-vaporized, ionized with electron impact at 70 eV. Ions are detected by a quadrupole mass spectrometer with a scan rate and m/z window of $500\,ms\,amu^{-1}$ and [10; 150], respectively. As described by Ng et al. (2011), instrument mass calibration was performed by injecting generated mono-disperse 300 nm ammonium nitrate particles into both ACSM and CPC, and assuming a particle density of $1.72\,g\,cm^{-3}$ and a shape factor of 0.8, the response factor (RF) of nitrate and relative response factor of ammonium could be calculated. Performed in November 2011, i.e. 3 months before the start of this study, the RF of nitrate and the relative ionization efficiency (RIE) of ammonium were $2.31 \times 10^{-11}\,A\,\mu g^{-1}\,m^{-3}$ and 6.0, respectively. Twenty scans (ten scans at ambient conditions, ten "blank" scans with filtered air) allowed for the continuous measurement of the concentrations of total non-refractory organics, nitrate, sulfate, ammonium, and chloride every 29 min.

Aerosol light absorption coefficients (b_{abs}) were obtained every 5 min at seven different wavelengths (370, 470, 520, 590, 660, 880 and 950 nm) using a Magee Scientific Aethalometer (model AE31) equipped with a $PM_{2.5}$ cut-off inlet. This instrument was operated at a flow rate of 5 L min^{-1}. Due to the methodology used within the Aethalometer (filter-based measurement), absorption coefficients directly obtained from this instrument are affected by various sampling and analytical artefacts (mostly referred as multiple scattering and loading effects) which need to be carefully compensated (Collaud Coen et al., 2010). In the present work, the correction procedure introduced by Weingartner et al. (2003) was applied to our dataset, as fully described in Sciare et al. (2011). Multi-wavelength absorption measurements were then used to apportion BC to two main fractions: fossil fuel BC (BC_{ff}) and wood burning BC (BC_{wb}), following the "Aethalometer model" methodology (Appendix A, in Supplement) introduced by Sandradewi et al. (2008) and successfully applied to the same instrument and at the same site one year earlier than the present study (Sciare et al., 2011). Consistency of such a deconvolution is illustrated by a good correlation between BC_{wb} and m/z 60 from the ACSM ($r^2 = 0.73$, $N = 2040$).

The consistency of ACSM and AE31 measurements has been checked performing 3 h PM_1 chemical mass closure obtained through the comparison of the sum of individual chemical species monitored using both instruments with total PM_1 concentrations measured independently using a co-located TEOM-FDMS. This comparison shows a slope of 0.99 and a correlation coefficient of 0.65 ($N = 394$ with 3 h averaged data), validating the combination (and the calibration) of both ACSM and AE31 instruments to accurately characterize the major chemical components of the PM_1 mass.

2.2 Source apportionment methods

Developed about 20 years ago (Paatero and Tapper, 1994), PMF is nowadays intensively used for the source apportionment of atmospheric PM pollutants using filter-based as well as on-line measurements. Briefly, time series of chemical species (or organic mass spectra for ACSM data) arranged as a matrix (**X**), are factorized into a linear combination of a factor (i.e. source profile) and timeserie sub-matrices (**F** and **G** respectively) following:

$$x_{ij} = \sum_{p} g_{ip} f_{pj} + e_{ij}, \tag{1}$$

where x_{ij} correspond to the elements of matrix **X**, p represents the number of factors in the solution, g_{ip} and f_{pj} correspond to the element of matrices **G** and **F** representing respectively time series and profiles (mass spectra for ACSM) of each factor, and e_{ij} correspond to residuals not fitted by the model for each data point. **G** and **F** matrices are resolved for a minimum value of Q, defined as:

$$Q = \sum_{i} \sum_{j} \left(\frac{e_{ij}^2}{\sigma_{ij}^2} \right), \tag{2}$$

where σ_{ij} represents the measurement uncertainty of each data point.

The analysis of ACSM organic mass spectra was performed using SourceFinder (SoFi v4.5, http://www.psi.ch/acsm-stations/me-2). This toolkit, implemented along with AMS and ACSM data processing software in Igor Pro (Wavemetrics, Inc.), was recently developed by Canonaco et al. (2013). It allows users to take advantage of the Multilinear-Engine (ME-2) algorithm (Paatero and Hopke, 2003), where a priori information might be introduced in form of known factor profiles and/or factor time series into the PMF analysis (Lanz et al., 2008). In this study the *a* value technique of the ME-2 solver was employed, where the constrained factor profiles were allowed to vary

Title Page
Abstract | Introduction
Conclusions | References
Tables | Figures
◀I | ▶I
◀ | ▶
Back | Close
Full Screen / Esc
Printer-friendly Version
Interactive Discussion

within the scalar value “a” (Eq. 3).

$$f_{j,\text{solution}} = f_j \pm a \cdot f_j \tag{3}$$

where f represents one factor profile in the **F** matrix.

Timeseries and uncertainty matrices were both obtained from the ACSM data analysis software (acsm_local Igor procedure v1520) (Zhang et al., 2005; Ng et al., 2011; Ulbrich et al., 2009). In our study, the two matrices contain 73 mass fragments (m/z), from $m/z = 12$ to $m/z = 100$, and 2040 samples. Previous AMS measurements performed in Paris (Crippa et al., 2013b, c) offered the opportunity to implement a priori factor profiles specifically representative of the Ile-de-France wintertime pollution; HOA and BBOA factor profiles were retrieved from the AMS spectral database (http://cires.colorado.edu/jimenez-group/AMSsd/, Ulbrich et al., 2009). The model was run several times, testing several numbers of (unconstrained) factors and a values, as presented in the Appendices B–D of the Supplement. The best solutions are presented and discussed in Sect. 3.2.

The second step of the source apportionment strategy presented here consists of a PM_1 source apportionment using outputs of the preliminary OA source apportionment described above, source specific black carbon concentrations from the Aethalometer model (BC_{wb} and BC_{ff}) and inorganic species (SO_4^{2-}, NO_3^-, NH_4^+, Cl^-) from ACSM measurements. This was performed using the EPA PMF software v3.0 (http://www.epa.gov/heasd/research/pmf.html, Norris et al., 2008). Based on the ME-2, this model has been extensively used for source apportionment from off-line measurements (Viana et al., 2008). Two approaches are available in the EPA software to input the uncertainty matrix; one can either input a predetermined uncertainty matrix, or only Limits Of Detection (LOD) and relative uncertainties (u in %) for each variable, where the final uncertainty U_{ij} for the ith specie at jth row is eventually calculated following

Polissar et al., 1998 (Eq. 4):

$$U_{ij} = \begin{cases} \frac{5}{6} \cdot \mathrm{LOD}_i & \text{if } C_j \leq \mathrm{LOD}_i \\ \sqrt{u_i^2 \cdot C_j^2 + \mathrm{LOD}_i^2} & \text{if } C_j > \mathrm{LOD}_i \end{cases} \tag{4}$$

Uncertainties of the concentrations of ACSM inorganic species from mass spectra were largely underestimated in the version of the ACSM analysis package used here, resulting in signal-to-noise ratios (S/N) which were too high for use in PMF analysis (Paatero and Hopke, 2003). Therefore, they were eventually obtained using the Polissar approach (Eq. 4). Moreover, the use of a single methodology for uncertainty calculations has the advantage to lead to a homogeneous error matrix. LODs for the inorganic species were calculated as 3 times the standard deviation calculated during a 3 day period, where a total filter was inserted at the ACSM inlet (Table 1). For OA PMF outputs, LODs and relative uncertainties were empirically determined in order to give enough weight to organic matter in the second PMF analysis. Their relative uncertainties were set to 30 %, assuming that previous PMF analysis should add additional errors due to residuals. For $\mathrm{BC_{wb}}$ and $\mathrm{BC_{ff}}$, a relative uncertainty of 40 % was used, accounting for an extended uncertainty from the Weingartner correction (Favez et al., 2009) and alpha uncertainty from possible absorption of wood-burning SOA at low wavelengths (Saleh et al., 2013). A relative uncertainty of 50 % was set for potassium due to possible measurement artifacts with $\mathrm{C_3H_3^+}$ fragment. An investigation of the impacts of uncertainty changes is described in Appendix E of the Supplement.

EPA PMF v3.0 also allows the empirical implementation of additional uncertainties following signal-to-noise ratios (Paatero and Hopke, 2003). Usually, species with a S/N ratio below 0.2, between 0.2 and 2, or greater than 2 are respectively considered as “bad”, “weak”, or “strong”. “Bad” variables are excluded from the dataset; “weak” variables get their uncertainties tripled, while uncertainties of “strong” variables stay unchanged. In the present study, all variables were considered as “strong”, except for chloride and potassium, set as “weak” as they exhibit low S/N ratios and aren’t specific tracers of a given emission source.

2.3 Non-parametric Wind Regression analysis

In an attempt to assign a geographical origin to the main sources of submicron aerosols and to perform a cross-validation of these results, a Non-parametric Wind Regression analysis (NWR) was performed on PMF^2 outputs. Developed by Henry et al. (2009), the NWR is a source-to-receptor model using kernel smoothing methods to estimate the average concentration of a pollutant given wind directions and wind speeds. The objective of NWR is thus to calculate $E(\theta|\vartheta)$, the smoothed concentration field of the pollutant given any predictor variable coordinates (θ, ϑ) representing wind direction and wind speed (Eq. 5).

$$E(\theta|\vartheta) = \frac{\sum_{i=1}^{N} K_1\left(\frac{\theta - W_i}{\sigma}\right) \cdot K_2\left(\frac{\vartheta - Y_i}{h}\right) \cdot C_i}{\sum_{i=1}^{N} K_1\left(\frac{\theta - W_i}{\sigma}\right) \cdot K_2\left(\frac{\vartheta - Y_i}{h}\right)} \tag{5}$$

where C_i, W_i and Y_i are the measured concentration, wind direction and wind speed at t_i; σ and h, the smoothing parameters; and K_1 and K_2 the two kernel functions defined as:

$$K_1(x) = \frac{1}{\sqrt{2\pi}} \cdot e^{-0.5 \cdot x^2}, \quad -\infty < x < \infty \tag{6}$$

$$K_2(x) = 0.75 \cdot (1 - x^2), \quad -1 < x < 1 = 0 \tag{7}$$

Smoothing parameters σ and h can be calculated using Gaussian distribution equations (Full Width at Half Maximum), but their empirical determination leads to similar results, since reasonable variations from their theoretical values do not change the final interpretation.

Meteorological data used for NWR were obtained from continuous 1 min measurements carried out on the campus of the Polytechnic School (4 km east of measurement

Title Page
Abstract | Introduction
Conclusions | References
Tables | Figures
◀| |▶
◀ ▶
Back | Close
Full Screen / Esc
Printer-friendly Version
Interactive Discussion

site) with an A100R Campbell Scientific anemometer and a W200P Campbell Scientific weathervane at 25 m above ground level (a.g.l.), above any impediment (e.g. trees or buildings) that could affect the measurement of a particular wind sector.

3 Results and discussion

3.1 Temporal trends of aerosol chemical composition

During the late 2012 winter, average PM_1 chemical composition (Fig. 2a) was clearly dominated by organic matter and secondary inorganic salts (mostly ammonium nitrate), which is fully consistent with the wintertime $PM_{2.5}$ chemical composition reported by Bressi et al. (2013) for the Paris region.

Three distinct periods (I, II and III) were considered here (Fig. 2a and b). The first period, from 30 January to 19 February is characterized by high concentrations of organic matter and BC_{wb} (44 % and 5.5 % on average, respectively), low temperatures (−1.9 °C on average, and below 0 °C all day long during the two-third of the period) and wind originating essentially from the NNW–NNE sector. A very intense organic peak is observed on the 5 February, and reaches maximum concentration (of about 70 $\mu g\,m^{-3}$) at 23:00 UTC. Along with high organic loading, a significant amount of BC_{wb} is also observed during that period, suggesting an intense wood burning emission episode. In addition, combined with low temperatures (below 0 °C), which increase domestic heating emissions, low wind speeds enable the accumulation of local pollutants within the boundary layer, exacerbating measured concentrations. The influence of this intense episode to the results of the PMF^2 analysis is investigated in Appendix F (in Supplement).

The second period, from 19 February to 10 March, exhibits lower PM concentrations (15 $\mu g\,m^{-3}$ on average), higher ambient temperatures and lower atmospheric pressure. Minor BC_{wb} and BC_{ff} peaks are observed (e.g. on 20, 27, 29 February) and associated with low wind speeds from the N–NNE sector, suggesting an influence of (local) combustion sources from Paris city.

The third period, from 10 March to 26 March, is characterized by the highest temperatures and daily temperature amplitudes (maximum of 15 °C in one day) along with dynamic winds blowing from all directions with an SW–NE axis. Also, higher PM concentrations with a significantly enhanced role of ammonium nitrate are observed, which, in these atmospheric conditions, is related to its gas-particle partitioning.

3.2 Preliminary OA source apportionment

As explained above, the first step of the PMF^2 analysis was conducted using SoFi constraining both HOA and primary BBOA (pBBOA) factor profiles which remain difficult to differentiate (Lanz et al., 2007). This constrained analysis was carried out with *a* value of 0.05 and 0.1 for HOA and pBBOA reference profiles, respectively, and remaining factors staying unconstrained. The three-factor solution presented in Fig. 3, gave most satisfactory results. As presented in Appendix B (in Supplement), any higher number of factors led to unstable solutions. Outputs from constrained analysis were largely consistent with preliminary unconstrained PMF outputs (Appendix C, in Supplement) and ranging *a* values from 0.05 to 0.80 for HOA and/or pBBOA reference profiles within the constrained analysis also exhibits quite stable solutions (Appendix D, in Supplement). It is also to note that COA could note be clearly deconvolved in this study, although it has been identified with previous AMS measurements at SIRTA by Crippa et al. (2013b), essentially due to lower sensitivity and narrower m/z scan range from ACSM measurements.

Based on the ME-2 outputs, OOA represents up to 78 % of the average organic mass (Fig. 4a), in good agreement with worldwide and European OOA high proportions (Zhang et al., 2007; Lanz et al., 2010). The contributions of HOA and pBBOA were 9.9 % and 12.3 %, respectively, on average, which is consistent with results obtained for Paris urban background conditions during winter 2009 (10–15 % for each factors) by applying PMF analysis to AMS organic mass spectra (Crippa et al., 2013b).

As expected, diurnal variations obtained for the three factors (Fig. 4b) indicate predominant nighttime contributions for pBBOA and OOA (mainly due to the subsidence of the boundary layer height and the condensation of semi-volatile material in the particulate phase at low temperatures) and increases of HOA during traffic peaks. These diurnal profiles are also in good agreement with those obtained using AMS-PMF during wintertime in the region of Paris (Crippa et al., 2013b). We thus conclude that outputs chosen for the present source apportionment are representative of those typically obtained from AMS (or ACSM)-PMF analysis.

Conceptually speaking and applied to OA mass spectra, this model only gathers m/z fragments into factors regarding the chemical structures of parent organic molecules (hydrocarbons, carboxylic acids, aromatics, ketones etc.), and thus does not lead to direct information of pollution sources. The organic chemical composition of aerosol pollution sources may indeed not be limited to one kind of molecular structure. Here, the high temporal correlation between pBBOA and HOA (r^2 = 0.85 for the whole campaign, but down to 0.55 when discarding the intense local wood smoke event on 6 February) contrasts with the poor correlation between $\mathrm{BC_{wb}}$ and $\mathrm{BC_{ff}}$ (r^2 = 0.09), and thus could suggest a common source of pBBOA and HOA. In this respect, combining the obtained OA factors with inorganic species and specific combustion tracers (BC constituents) in a second PMF analysis could allow for the apportionment of the main submicron aerosol sources and processes.

Nevertheless, as PMF model does not necessarily reconstruct the input data perfectly: residuals could then still contain some pieces of information, and could increase the uncertainty of the outputs, potentially leading to erroneous results from a subsequent PMF analysis. Here, residuals of key variables (m/z 43, 44, 55, 57 and 60) all follow an unimodal Gaussian distribution centered at zero (Fig. 5a). Moreover, the sum of all organic m/z (row-wise) was compared to the sum of OA factors (HOA, BBOA and OOA). The regression (Fig. 5b) shows a slope very close to 1 (1.01) and a very satisfactory r^2 (> 0.99). This highlights the fact that (i) Q and residuals were satisfactorily minimized; (ii) no significant information remain unaccounted from this OA PMF analysis; (iii) in our case, residuals from this OA PMF analysis as it has been performed would have little weight in the subsequent PMF calculation.

3.3 PM_1 source apportionment and geographical origins

PM_1 source apportionment (i.e. the second step of the PMF^2 methodology) was carried out using US EPA PMF v3.0 in order to allow bootstrap analyses (this option being unavailable so far using SoFi v4.5). The optimal number of factors was determined using atmospheric relevance of factor profiles and then bootstrap analysis. The four-factor solution featured the most stable and realistic results with very satisfactory bootstrap analysis (Table 2), and was used to identify two factors corresponding to distinct pollution sources, biomass and fossil fuel combustion; and two factors relative to secondary material characterized by one of their physical properties, semi-volatile and low-volatile secondary aerosols. Factor profiles and time series are presented in Fig. 6.

3.3.1 Wood-burning factor

The wood-burning factor includes significant contributions from pBBOA, HOA, and OOA. For pBBOA and BC_{wb}, respectively, 90 % and 85 % of the total mean concentration fall within the wood-burning factor. This factor also accounts for 30 % of total HOA (Fig. 9), which is in accordance with the fact that HOA concentrations were found to be present within wood burning emissions of combustion processes (DeCarlo et al., 2010; Poulain et al., 2011). The very high concentration of OOA in this factor suggests that the secondary organic material is associated with wood burning, possibly originating from condensation of VOCs and atmospheric ageing (SOA and OPOA formation, respectively). This is consistent with recent laboratory studies (May et al., 2013) showing that the majority of biomass burning POA is semi-volatile and emphasizing the role of fast SOA formation processes from Intermediate VOCs.

The average OM_{wb}-to-BC_{wb} ratio calculated here is 10.3 (where OM_{wb} equals the sum of the concentration of the three organic constituents in the wood-burning factor).

When assuming that OOA in this factor is only secondary, the $OM_{wb\_primary}$-to-BC_{wb} ratio decreases to 4.7 (where $OM_{wb\_primary} = OM_{wb} - OOA_{wb}$). Part of wood burning OOA could be considered as primary (Weimer et al., 2008; Grieshop et al., 2009; Heringa et al., 2011) but its apportionment remains very challenging due to the lack of identification of specific secondary organic tracers.

Using the PMF^2 methodology introduced here, the average contribution of the wood burning source to total OA is found to be of about 35 % during the present study. This contribution is very consistent with the one obtained for Paris urban background conditions during winter 2009 (about 30 %) when applying PMF analysis to combined AMS and PTR-MS (Proton-Transfer Reaction Mass Spectrometer) organic mass spectra (Crippa et al., 2013b). Indeed, the use of additional tracers (VOCs or BC_{wb} and BC_{ff}) leads to a better characterization of wood burning emissions, especially by taking into account secondary related organic material (Fig. 10). The wood burning factor contributes up to 17 % to the PM_1 mass on average (Fig. 7b), but significant sporadic episodes are noticeable, especially on 2 and 12 February, rising to 66 % and 38 % of PM_1, respectively. Wind regression (Fig. 8) highlights clear local emissions with high concentrations linked to low wind speeds (below 5 km h^{-1}), underlining the significance of local wood burning emissions to wintertime pollution events.

3.3.2 Fossil fuel combustion factor

A fossil fuel combustion factor was identified accounting for, on average, 11 % of the total PM_1 mass (Fig. 6b). This factor includes strong contributions from HOA and BC_{ff} concentrations (60 % and 80 %, respectively) (Fig. 6). The predominance of traffic emissions within this factor is highlighted by its diurnal variation, in phase with traffic peaks (Fig. 7a).

Another striking feature is that OOA represents about half of OA in this profile (Fig. 9). While primary traffic emissions of OOA are unlikely to be predominant, fast oxidation and condensation processes (Chirico et al., 2011; Carbone et al., 2013) could explain the high concentrations of OOA in this factor. It is however important to note that small changes in OA uncertainty (in the 30–40 % range, referring to Appendix E, in Supplement) lead to discrepancies in the proportion of OOA within $OM_{traffic}$, but remains always higher than 25 %. The OM_{ff}-to-BC_{ff} ratio of 1.15 found here is very consistent with the ratio of 1.05 obtained from measurements carried out in September 2012 in a highway-tunnel near Paris (Petit et al., unpublished data), although tunnel measurements can be impacted by gas-particle partitioning (Chirico et al., 2010, 2011). Despite challenging uncertainties of these results, these two features particularly highlight the presence of secondary organic material from traffic emissions in ambient measurements. Ammonium and nitrate in this factor (in stoichiometric proportion) suggest condensation of these species with mobile emissions, as previously highlighted in the region of Paris by Healy et al. (2013). Wind regression shows clear local emissions (high concentrations at low wind speed), and additionally a diffuse concentration field from the directions between the North and the East. This suggests the transport of traffic carbonaceous emissions with ammonium nitrate or its gaseous precursor (NH_3, HNO_3/NO_x) over the Ile-de-France region (the influence of Paris city emissions cannot be highlighted with this method) (Fig. 8).

3.3.3 Semi-volatile secondary aerosol

The semi-volatile secondary aerosol factor is characterized by a large contribution from (semi-volatile) ammonium nitrate and, to a lesser extent, of OOA (76 % and 23 % of mass in factor, respectively) (Fig. 6). This factor is found to represent about 57 % of PM_1 (Fig. 7b). The nitrate appears to be fully neutralized by ammonium (only 2 % of cation excess).

Temporal variations show a clear diurnal pattern (Fig. 7a), with a decrease of concentrations during the afternoon linked to the gas-phase partitioning of condensed semi-volatile material following ambient temperature variations. Since atmospheric (trans)formation pathways of secondary organic and inorganic aerosols are different, no thorough assessments can be undertaken to link the amount of OOA in this factor profile to a specific atmospheric process or source; here the OOA should only be characterized as mainly semi-volatile.

The NWR for this factor exhibits two distinct hotspots in the N and NNE wind sector at wind speeds above 10 km h^{-1}; as well as a diffuse signal between the aforementioned wind sectors; highlighting probable trans-boundary transport from highly industrialized regions upwind of the region of Paris (Belgium, the Netherlands and Western-Germany) (Fig. 8). This result is in accordance with (i) the European concentration distribution of nitrogen oxides, nitric acid and ammonia, reported by Pay et al. (2012); (ii) previous PMF analysis identifying an ammonium nitrate rich factor in this region of France (Waked et al., 2014; Bressi et al., 2013b); and (iii) the Lenshow methodology (Lenschow et al., 2001) applied in Paris (Ghersi et al., 2012).

3.3.4 Low-volatility secondary aerosol

The last identified factor is assigned as low-volatility secondary aerosol and accounts for 15 % of the total PM_1 on average. This factor contains most of the sulfate as well as significant amounts of ammonium, OOA, and some nitrate. It also includes half of total non-refractory chloride, suggesting secondary aerosols from industrial emissions. Moreover, the presence of primary aerosols in the factor profile, especially BC_{ff}, suggests that part of BC_{ff} is internally mixed with secondary organic aerosols and sulfates.

The diurnal cycle shows a rather flat pattern, as less volatile oxidized aerosols do not evaporate at ambient temperatures (by definition) (Fig. 7a). Wind regression allows the identification of a very specific hotspot located in the NE wind sector at wind speeds above 20 km h^{-1} (Fig. 8). At lower wind speeds, a diffuse but significant signal appears in NW wind sector. These two sectors are well known to contribute to sulfur dioxide emissions through (i) a dense network of petrochemical cracking facilities, and (ii) intense shipping traffic in the English Channel (Pay et al., 2012; Waked et al., 2014; Bressi et al., 2013b). Long-range transport is also consistent with a low degree of diurnal variation. As for the semi-volatile secondary aerosol factor, it should be noted that it is not expected that organic and inorganic species exhibit constant ratio during time. This kind of approximation is however inherent to PMF analysis, even if a better separation of the different type of inorganic/organic aerosols may be achieved through the use of high-resolution mass spectrometry and/or specific organic and elemental tracers (which were not available here).

4 Conclusion

We are using here a novel methodology to perform the source apportionment of PM_1 from near real-time data. This method has been applied to wintertime pollution in the Paris region from early February to late March 2012. First, high time resolution organic aerosol concentrations were measured by ACSM and statistically analyzed by PMF in order to investigate sources and transformation processes of OA. This OA source apportionment led to the identification of three factors that are commonly observed in industrialized regions during winter (HOA, pBBOA and OOA). However, the two combustion OA factors (HOA and pBBOA) seem to share a common source as suggested by the simultaneous correlation of HOA with BC_{wb} and BC_{ff}. Instead of only documenting poor or satisfactory correlations between OA factors and external tracers, co-variations were more thoroughly investigated through a second factorization analysis step.

A second PMF analysis, including OA factors, inorganic species and black carbon constituents (BC_{ff} and BC_{wb}) were then achieved to investigate major sources of submicron aerosols, leading to a considerably improved characterization of local and regional signal combustion sources. Wood burning was found to significantly contribute to HOA and OOA, characterizing primary and secondary related wood burning contributions in a single source specific factor. Therefore, pBBOA remains a specific tracer of biomass burning, but does not fully represent the total contribution to the mass of this source. HOA, commonly used as a tracer of traffic, is found here to also originate from wintertime local wood burning emissions. Finally, OOA is found to significantly contribute to the traffic organic mass although its exact contribution cannot be determined without the much-needed thorough determination of uncertainties.

This methodology is especially efficient when characterizing the mass of wintertime PM_1 pollution sources in urban areas and helped to strengthen the bonds between OA factors and pollution sources. To our knowledge, this is the first time that two consecutive PMF analyses have been performed in order to optimize the characterization of PM_1 pollution sources. This methodology shares the same goal than innovative approaches including inorganic compounds, as recently proposed for measurements obtained using high resolution AMS (Sun et al., 2012; Crippa et al., 2013c; McGuire et al., 2014). It also allows distributing OA factors usually obtained from PMF analysis applied to organic mass spectra to more specific PM_1 sources. Furthermore, similarly to the methodology proposed by Crippa et al. (2013b) for AMS and PTR-MS datasets, such an approach may offer various interesting possibilities for future analyses, such as the inclusion of on-line measurements of metals to apportion specific sources (e.g. shipping, petrochemical facilities, smelters) or size distribution information to identify and/or characterize transformation processes. Finally, uncertainties need to be better refined and thoroughly estimated, through the use of (i) timeserie bootstrapping for OA factors and (ii) recently developed AE33 Aethalometer, automatically correcting for absorption artifacts and potentially leading to decreased uncertainties.

The Supplement related to this article is available online at doi:10.5194/acpd-14-14159-2014-supplement.

Acknowledgements. The research leading to the these results has received funding from INERIS, the European Union Seventh Framework Program (FP7/2007–2013) project ACTRIS under grant agreement no. 262254, the DIM-R2DS program for the funding of the ACSM equipment, the PRIMEQUAL PREQUALIF program for long term observations of Black Carbon.

References

Adler, G., Flores, J. M., Abo Riziq, A., Borrmann, S., and Rudich, Y.: Chemical, physical, and optical evolution of biomass burning aerosols: a case study, Atmos. Chem. Phys., 11, 1491–1503, doi:10.5194/acp-11-1491-2011, 2011.

Allan, J. D., Williams, P. I., Morgan, W. T., Martin, C. L., Flynn, M. J., Lee, J., Nemitz, E., Phillips, G. J., Gallagher, M. W., and Coe, H.: Contributions from transport, solid fuel burning and cooking to primary organic aerosols in two UK cities, Atmos. Chem. Phys., 10, 647–668, doi:10.5194/acp-10-647-2010, 2010.

Bressi, M., Sciare, J., Ghersi, V., Bonnaire, N., Nicolas, J. B., Petit, J.-E., Moukhtar, S., Rosso, A., Mihalopoulos, N., and Féron, A.: A one-year comprehensive chemical characterisation of fine aerosol ($PM_{2.5}$) at urban, suburban and rural background sites in the region of Paris (France), Atmos. Chem. Phys., 13, 7825–7844, doi:10.5194/acp-13-7825-2013, 2013a.

Bressi, M., Sciare, J., Ghersi, V., Mihalopoulos, N., Petit, J.-E., Nicolas, J. B., Moukhtar, S., Rosso, A., Féron, A., Bonnaire, N., Poulakis, E., and Theodosi, C.: Sources and geographical origins of fine aerosols in Paris (France), Atmos. Chem. Phys. Discuss., 13, 33237–33309, doi:10.5194/acpd-13-33237-2013, 2013b.

Canonaco, F., Crippa, M., Slowik, J. G., Baltensperger, U., and Prévôt, A. S. H.: SoFi, an IGOR-based interface for the efficient use of the generalized multilinear engine (ME-2) for the source apportionment: ME-2 application to aerosol mass spectrometer data, Atmos. Meas. Tech., 6, 3649–3661, doi:10.5194/amt-6-3649-2013, 2013.

Carbone, S., Saarikoski, S., Frey, A., Reyes, F., Reyes, P., Castillo, M., Gramsch, E., Oyola, P., Jayne, J. T., Worsnop, D. R., and Hillamo, R.: Chemical characterization of submicron aerosol particles in Santiago de Chile, Aerosol Air Qual. Res., 13, 462–473, doi:10.4209/aaqr.2012.10.0261, 2013.

Chirico, R., DeCarlo, P. F., Heringa, M. F., Tritscher, T., Richter, R., Prévôt, A. S. H., Dommen, J., Weingartner, E., Wehrle, G., Gysel, M., Laborde, M., and Baltensperger, U.: Impact of aftertreatment devices on primary emissions and secondary organic aerosol formation potential from in-use diesel vehicles: results from smog chamber experiments, Atmos. Chem. Phys., 10, 11545–11563, doi:10.5194/acp-10-11545-2010, 2010.

Chirico, R., Prevot, A. S. H., DeCarlo, P. F., Heringa, M. F., Richter, R., Weingartner, E., and Baltensperger, U.: Aerosol and trace gas vehicle emission factors measured in a tunnel using an Aerosol Mass Spectrometer and other on-line instrumentation, Atmos. Environ., 45, 2182–2192, doi:10.1016/j.atmosenv.2011.01.069, 2011.

Collaud Coen, M., Weingartner, E., Apituley, A., Ceburnis, D., Fierz-Schmidhauser, R., Flentje, H., Henzing, J. S., Jennings, S. G., Moerman, M., Petzold, A., Schmid, O., and Baltensperger, U.: Minimizing light absorption measurement artifacts of the Aethalometer: evaluation of five correction algorithms, Atmos. Meas. Tech., 3, 457–474, doi:10.5194/amt-3-457-2010, 2010.

Crippa, M., Canonaco, F., Lanz, V. A., Äijälä, M., Allan, J. D., Carbone, S., Capes, G., Dall'Osto, M., Day, D. A., DeCarlo, P. F., Di Marco, C. F., Ehn, M., Eriksson, A., Freney, E., Hildebrandt Ruiz, L., Hillamo, R., Jimenez, J.-L., Junninen, H., Kiendler-Scharr, A., Kortelainen, A.-M., Kulmala, M., Mensah, A. A., Mohr, C., Nemitz, E., O'Dowd, C., Ovadnevaite, J., Pandis, S. N., Petäjä, T., Poulain, L., Saarikoski, S., Sellegri, K., Swietlicki, E., Tiitta, P., Worsnop, D. R., Baltensperger, U., and Prévôt, A. S. H.: Organic aerosol components derived from 25 AMS datasets across Europe using a newly developed ME-2 based source apportionment strategy, Atmos. Chem. Phys. Discuss., 13, 23325–23371, doi:10.5194/acpd-13-23325-2013, 2013a.

Crippa, M., Canonaco, F., Slowik, J. G., El Haddad, I., DeCarlo, P. F., Mohr, C., Heringa, M. F., Chirico, R., Marchand, N., Temime-Roussel, B., Abidi, E., Poulain, L., Wiedensohler, A., Baltensperger, U., and Prévôt, A. S. H.: Primary and secondary organic aerosol origin by combined gas-particle phase source apportionment, Atmos. Chem. Phys., 13, 8411–8426, doi:10.5194/acp-13-8411-2013, 2013b.

Crippa, M., El Haddad, I., Slowik, J. G., DeCarlo, P. F., Mohr, C., Heringa, M. F., Chirico, R., Marchand, N., Sciare, J., Baltensperger, U., and Prevot, A. S. H.: Identification of marine and continental aerosol sources in Paris using high resolution aerosol mass spectrometry, J. Geophys. Res.-Atmos., 118, 1950–1963, doi:10.1002/jgrd.50151, 2013c.

DeCarlo, P. F., Ulbrich, I. M., Crounse, J., de Foy, B., Dunlea, E. J., Aiken, A. C., Knapp, D., Weinheimer, A. J., Campos, T., Wennberg, P. O., and Jimenez, J. L.: Investigation of the sources and processing of organic aerosol over the Central Mexican Plateau from aircraft measurements during MILAGRO, Atmos. Chem. Phys., 10, 5257–5280, doi:10.5194/acp-10-5257-2010, 2010.

Favez, O., Cachier, H., Sciare, J., Sarda-estève, R., and Martinon, L.: Evidence for a significant contribution of wood burning aerosols to $PM_{2.5}$ during the winter season in Paris, France, Atmos. Environ., 43, 3640–3644, 2009.

Favez, O., El Haddad, I., Piot, C., Boréave, A., Abidi, E., Marchand, N., Jaffrezo, J.-L., Besombes, J.-L., Personnaz, M.-B., Sciare, J., Wortham, H., George, C., and D'Anna, B.: Intercomparison of source apportionment models for the estimation of wood burning aerosols during wintertime in an Alpine city (Grenoble, France), Atmos. Chem. Phys., 10, 5295–5314, doi:10.5194/acp-10-5295-2010, 2010.

Favez, O., Petit, J.-E., Bessagnet, B., Meleux, F., Chiappini, L., Lemeur, S., Labartette, C., Chappaz, C., Guergnion, P.-Y., Saison, J.-Y., Chretien, E., Pallares, C., Verlhac, S., Aujay, R., Malherbe, L., Beauchamp, M., Piot, C., Jaffrezo, J.-L., Besombes, J.-L., Sciare, J., Rouïl, L., and Leoz-Garziandia, E.: Main properties and origines of winter PM_{10} pollution events in France, Pollut. Atmos., Special Issue, 163–182, 2012.

Freutel, F., Schneider, J., Drewnick, F., von der Weiden-Reinmüller, S.-L., Crippa, M., Prévôt, A. S. H., Baltensperger, U., Poulain, L., Wiedensohler, A., Sciare, J., Sarda-Estève, R., Burkhart, J. F., Eckhardt, S., Stohl, A., Gros, V., Colomb, A., Michoud, V., Doussin, J. F., Borbon, A., Haeffelin, M., Morille, Y., Beekmann, M., and Borrmann, S.: Aerosol particle measurements at three stationary sites in the megacity of Paris during summer 2009: meteorology and air mass origin dominate aerosol particle composition and size distribution, Atmos. Chem. Phys., 13, 933–959, doi:10.5194/acp-13-933-2013, 2013.

Ghersi, V., Rosso, A., Moukhtar, S., Léger, K., Sciare, J., Bressi, M., Nicolas, J., Féron, A., and Bonnaire, N.: Origine des particules fines ($PM_{2.5}$) en Ile-de-France, Pollus. Atmos., Special Issue, 188–198, November 2012.

Grieshop, A. P., Logue, J. M., Donahue, N. M., and Robinson, A. L.: Laboratory investigation of photochemical oxidation of organic aerosol from wood fires 1: measurement and simulation of organic aerosol evolution, Atmos. Chem. Phys., 9, 1263–1277, doi:10.5194/acp-9-1263-2009, 2009.

Haeffelin, M., Barthès, L., Bock, O., Boitel, C., Bony, S., Bouniol, D., Chepfer, H., Chiriaco, M., Cuesta, J., Delanoë, J., Drobinski, P., Dufresne, J.-L., Flamant, C., Grall, M., Hodzic, A., Hourdin, F., Lapouge, F., Lemaître, Y., Mathieu, A., Morille, Y., Naud, C., Noël, V., O'Hirok, W., Pelon, J., Pietras, C., Protat, A., Romand, B., Scialom, G., and Vautard, R.: SIRTA, a ground-based atmospheric observatory for cloud and aerosol research, Ann. Geophys., 23, 253–275, doi:10.5194/angeo-23-253-2005, 2005.

Haywood, J. and Boucher, O.: Estimates of the direct and indirect radiative forcing due to tropospheric aerosols: a review, Rev. Geophys., 38, 513–543, 2000.

Healy, R. M., Sciare, J., Poulain, L., Crippa, M., Wiedensohler, A., Prévôt, A. S. H., Baltensperger, U., Sarda-Estève, R., McGuire, M. L., Jeong, C.-H., McGillicuddy, E., O'Connor, I. P., Sodeau, J. R., Evans, G. J., and Wenger, J. C.: Quantitative determination of carbonaceous particle mixing state in Paris using single-particle mass spectrometer and aerosol mass spectrometer measurements, Atmos. Chem. Phys., 13, 9479–9496, doi:10.5194/acp-13-9479-2013, 2013.

Henry, R., Norris, G. A., Vedantham, R., and Turner, J. R.: Source region identification using kernel smoothing, Environ. Sci. Technol., 43, 4090–4097, doi:10.1021/es8011723, 2009.

Heringa, M. F., DeCarlo, P. F., Chirico, R., Tritscher, T., Dommen, J., Weingartner, E., Richter, R., Wehrle, G., Prévôt, A. S. H., and Baltensperger, U.: Investigations of primary and secondary particulate matter of different wood combustion appliances with a high-resolution time-of-flight aerosol mass spectrometer, Atmos. Chem. Phys., 11, 5945–5957, doi:10.5194/acp-11-5945-2011, 2011.

Jimenez, J. L., Canagaratna, M. R., Donahue, N. M., Prevot, A. S. H., Zhang, Q., Kroll, J. H., DeCarlo, P. F., Allan, J. D., Coe, H., Ng, N. L., Aiken, A. C., Docherty, K. S., Ulbrich, I. M., Grieshop, A. P., Robinson, A. L., Duplissy, J., Smith, J. D., Wilson, K. R., Lanz, V. A., Hueglin, C., Sun, Y. L., Tian, J., Laaksonen, A., Raatikainen, T., Rautiainen, J., Vaattovaara, P., Ehn, M., Kulmala, M., Tomlinson, J. M., Collins, D. R., Cubison, M. J., Dunlea, E. J., Huffman, J. A., Onasch, T. B., Alfarra, M. R., Williams, P. I., Bower, K., Kondo, Y., Schneider, J., Drewnick, F., Borrmann, S., Weimer, S., Demerjian, K., Salcedo, D., Cottrell, L., Griffin, R., Takami, A., Miyoshi, T., Hatakeyama, S., Shimono, A., Sun, J. Y., Zhang, Y. M., Dzepina, K., Kimmel, J. R., Sueper, D., Jayne, J. T., Herndon, S. C., Trimborn, A. M., Williams, L. R., Wood, E. C., Middlebrook, A. M., Kolb, C. E., Baltensperger, U., and Worsnop, D. R.: Evolution of organic aerosols in the atmosphere, Science, 326, 1525–1529, doi:10.1126/science.1180353, 2009.

Lanz, V. A., Alfarra, M. R., Baltensperger, U., Buchmann, B., Hueglin, C., and Prevot, A. S. H.: Source apportionment of submicron organic aerosols at an urban site by factor analytical modelling of aerosol mass spectra, Atmos. Chem. Phys., 7, 1503–1522, doi:10.5194/acp-7-1503-2007, 2007.

Lanz, V. A., Alfarra, M. R., Baltensperger, U., Buchmann, B., Hueglin, C., Szidat, S., Wehrli, M. N., Wacker, L., Weimer, S., and Caseiro, A.: Source attribution of submicron organic aerosols during wintertime inversions by advanced factor analysis of aerosol mass spectra, Environ. Sci. Technol., 42, 214–220, 2008.

Lanz, V. A., Prévôt, A. S. H., Alfarra, M. R., Weimer, S., Mohr, C., DeCarlo, P. F., Gianini, M. F. D., Hueglin, C., Schneider, J., Favez, O., D'Anna, B., George, C., and Baltensperger, U.: Characterization of aerosol chemical composition with aerosol mass spectrometry in Central Europe: an overview, Atmos. Chem. Phys., 10, 10453–10471, doi:10.5194/acp-10-10453-2010, 2010.

Lenschow, P., Abraham, H.-J., Kutzner, K., Lutz, M., Preuß, J.-D., and Reichenbächer, W.: Some ideas about the sources of PM_{10}, Atmos. Environ., 35, S23–S33, 2001.

May, A. A., Levin, E. J. T., Hennigan, C. J., Riipinen, I., Lee, T., Collett, J. L., Jimenez, J. L., Kreidenweis, S. M., and Robinson, A. L.: Gas-particle partitioning of primary organic aerosol emissions: 3. Biomass burning, J. Geophys. Res.-Atmos., 118, 11327–11338, doi:10.1002/jgrd.50828, 2013.

McGuire, M. L., Chang, R. Y.-W., Slowik, J. G., Jeong, C.-H., Healy, R. M., Lu, G., Mihele, C., Abbatt, J. P. D., Brook, J. R., and Evans, G. J.: Enhancing non-refractory aerosol apportionment from an urban industrial site through receptor modelling of complete high time-resolution aerosol mass spectra, Atmos. Chem. Phys. Discuss., 14, 5081–5145, doi:10.5194/acpd-14-5081-2014, 2014.

Ng, N. L., Herndon, S. C., Trimborn, A., Canagaratna, M. R., Croteau, P. L., Onasch, T. B., Sueper, D., Worsnop, D. R., Zhang, Q., and Sun, Y. L.: An aerosol chemical speciation monitor (ACSM) for routine monitoring of the composition and mass concentrations of ambient aerosol, Aerosol Sci. Tech., 45, 780–794, 2011.

Norris, G. A., Vedantham, R., Wade, K., Brown, S., Prouty, J., and Foley, C.: EPA Positive Matrix Factorization (PMF) 3.0: Fundamentals & User Guide, US Environmental Protection Agency, available at: http://www.epa.gov/heasd/documents/EPA_PMF_3.0_User_Guide.pdf (last access: 20 February 2014), 2008.

Paatero, P. and Hopke, P. K.: Discarding or downweighting high-noise variables in factor analytic models, Anal. Chim. Acta, 490, 277–289, 2003.

Paatero, P. and Tapper, U.: Positive matrix factorization: a non-negative factor model with optimal utilization of error estimates of data values, Environmetrics, 5, 111–126, doi:10.1002/env.3170050203, 1994.

Pay, M. T., Jiménez-Guerrero, P., and Baldasano, J. M.: Assessing sensitivity regimes of secondary inorganic aerosol formation in Europe with the CALIOPE-EU modeling system, Atmos. Environ., 51, 146–164, doi:10.1016/j.atmosenv.2012.01.027, 2012.

Platt, S. M., El Haddad, I., Zardini, A. A., Clairotte, M., Astorga, C., Wolf, R., Slowik, J. G., Temime-Roussel, B., Marchand, N., Ježek, I., Drinovec, L., Močnik, G., Möhler, O., Richter, R., Barmet, P., Bianchi, F., Baltensperger, U., and Prévôt, A. S. H.: Secondary organic aerosol formation from gasoline vehicle emissions in a new mobile environmental reaction chamber, Atmos. Chem. Phys., 13, 9141–9158, doi:10.5194/acp-13-9141-2013, 2013.

Polissar, A. V., Hopke, P. K., Paatero, P., Malm, W. C., and Sisler, J. F.: Atmospheric aerosol over Alaska: 2. Elemental composition and sources, J. Geophys. Res.-Atmos., 103, 19045–19057, doi:10.1029/98JD01212, 1998.

Pope, C. A. and Dockery, D. W.: Health effects of fine particulate air pollution: lines that connect, J. Air Waste Manag. Assoc., 56, 709–742, doi:10.1080/10473289.2006.10464485, 2006.

Pope, C. A., Hansen, M. L., Long, R. W., Nielsen, K. R., Eatough, N. L., Wilson, W. E., and Eatough, D. J.: Ambient particulate air pollution, heart rate variability, and blood markers of inflammation in a panel of elderly subjects, Environ. Health Persp., 112, 339–345, 2004.

Poulain, L., Iinuma, Y., Müller, K., Birmili, W., Weinhold, K., Brüggemann, E., Gnauk, T., Hausmann, A., Löschau, G., Wiedensohler, A., and Herrmann, H.: Diurnal variations of ambient particulate wood burning emissions and their contribution to the concentration of Polycyclic Aromatic Hydrocarbons (PAHs) in Seiffen, Germany, Atmos. Chem. Phys., 11, 12697–12713, doi:10.5194/acp-11-12697-2011, 2011.

Robinson, A. L., Subramanian, R., Donahue, N. M., Bernardo-Bricker, A., and Rogge, W. F.: Source apportionment of molecular markers and organic aerosol 2. Biomass smoke, Environ. Sci. Technol., 40, 7811–7819, doi:10.1021/es060782h, 2006.

Robinson, A. L., Donahue, N. M., Shrivastava, M. K., Weitkamp, E. A., Sage, A. M., Grieshop, A. P., Lane, T. E., Pierce, J. R., and Pandis, S. N.: Rethinking organic aerosols: semivolatile emissions and photochemical aging, Science, 315, 1259–1262, doi:10.1126/science.1133061, 2007.

Rosenfeld, D., Lohmann, U., Raga, G. B., O'Dowd, C. D., Kulmala, M., Fuzzi, S., Reissell, A., and Andreae, M. O.: Flood or drought: how do aerosols affect precipitation?, Science, 321, 1309–1313, 2008.

Sage, A. M., Weitkamp, E. A., Robinson, A. L., and Donahue, N. M.: Evolving mass spectra of the oxidized component of organic aerosol: results from aerosol mass spectrometer analyses of aged diesel emissions, Atmos. Chem. Phys., 8, 1139–1152, doi:10.5194/acp-8-1139-2008, 2008.

Saleh, R., Hennigan, C. J., McMeeking, G. R., Chuang, W. K., Robinson, E. S., Coe, H., Donahue, N. M., and Robinson, A. L.: Absorptivity of brown carbon in fresh and photo-chemically aged biomass-burning emissions, Atmos. Chem. Phys., 13, 7683–7693, doi:10.5194/acp-13-7683-2013, 2013.

Sandradewi, J., Prévôt, A. S. H., Szidat, S., Perron, N., Alfarra, M. R., Lanz, V. A., Weingartner, E., and Baltensperger, U.: Using aerosol light absorption measurements for the quantitative determination of wood burning and traffic emission contributions to particulate matter, Environ. Sci. Technol., 42, 3316–3323, doi:10.1021/es702253m, 2008.

Sciare, J., d' Argouges, O., Sarda-Estève, R., Gaimoz, C., Dolgorouky, C., Bonnaire, N., Favez, O., Bonsang, B., and Gros, V.: Large contribution of water-insoluble secondary organic aerosols in the region of Paris (France) during wintertime, J. Geophys. Res.-Atmos., 116, D22203, doi:10.1029/2011JD015756, 2011.

Sun, Y. L., Zhang, Q., Schwab, J. J., Yang, T., Ng, N. L., and Demerjian, K. L.: Factor analysis of combined organic and inorganic aerosol mass spectra from high resolution aerosol mass spectrometer measurements, Atmos. Chem. Phys., 12, 8537–8551, doi:10.5194/acp-12-8537-2012, 2012.

Ulbrich, I. M., Canagaratna, M. R., Zhang, Q., Worsnop, D. R., and Jimenez, J. L.: Interpretation of organic components from Positive Matrix Factorization of aerosol mass spectrometric data, Atmos. Chem. Phys., 9, 2891–2918, doi:10.5194/acp-9-2891-2009, 2009.

Viana, M., Kuhlbusch, T. A. J., Querol, X., Alastuey, A., Harrison, R. M., Hopke, P. K., Winiwarter, W., Vallius, M., Szidat, S., Prévôt, A. S. H., Hueglin, C., Bloemen, H., Wåhlin, P., Vecchi, R., Miranda, A. I., Kasper-Giebl, A., Maenhaut, W., and Hitzenberger, R.: Source apportionment of particulate matter in Europe: a review of methods and results, J. Aerosol Sci., 39, 827–849, doi:10.1016/j.jaerosci.2008.05.007, 2008.

Waked, A., Favez, O., Alleman, L. Y., Piot, C., Petit, J.-E., Delaunay, T., Verlinden, E., Golly, B., Besombes, J.-L., Jaffrezo, J.-L., and Leoz-Garziandia, E.: Source apportionment of PM_{10} in a north-western Europe regional urban background site (Lens, France) using positive matrix factorization and including primary biogenic emissions, Atmos. Chem. Phys., 14, 3325–3346, doi:10.5194/acp-14-3325-2014, 2014.

Weimer, S., Alfarra, M. R., Schreiber, D., Mohr, M., Prévôt, A. S. H., and Baltensperger, U.: Organic aerosol mass spectral signatures from wood-burning emissions: influence of burning conditions and wood type, J. Geophys. Res., 113, D10304, doi:10.1029/2007JD009309, 2008.

Weitkamp, E. A., Sage, A. M., Pierce, J. R., Donahue, N. M., and Robinson, A. L.: Organic aerosol formation from photochemical oxidation of diesel exhaust in a smog chamber, Environ. Sci. Technol., 41, 6969–6975, doi:10.1021/es070193r, 2007.

Zhang, Q., Alfarra, M. R., Worsnop, D. R., Allan, J. D., Coe, H., Canagaratna, M. R., and Jimenez, J. L.: Deconvolution and quantification of hydrocarbon-like and oxygenated organic aerosols based on aerosol mass spectrometry, Environ. Sci. Technol., 39, 4938–4952, doi:10.1021/es048568l, 2005.

Zhang, Q., Jimenez, J. L., Canagaratna, M. R., Allan, J. D., Coe, H., Ulbrich, I., Alfarra, M. R., Takami, A., Middlebrook, A. M., Sun, Y. L., Dzepina, K., Dunlea, E., Docherty, K., DeCarlo, P. F., Salcedo, D., Onasch, T., Jayne, J. T., Miyoshi, T., Shimono, A., Hatakeyama, S., Takegawa, N., Kondo, Y., Schneider, J., Drewnick, F., Borrmann, S., Weimer, S., Demerjian, K., Williams, P., Bower, K., Bahreini, R., Cottrell, L., Griffin, R. J., Rautiainen, J., Sun, J. Y., Zhang, Y. M., and Worsnop, D. R.: Ubiquity and dominance of oxygenated species in organic aerosols in anthropogenically-influenced Northern Hemisphere midlatitudes, Geophys. Res. Lett., 34, L13801, doi:10.1029/2007GL029979, 2007.

Zhang, Q., Jimenez, J. L., Canagaratna, M. R., Ulbrich, I. M., Ng, N. L., Worsnop, D. R., and Sun, Y.: Understanding atmospheric organic aerosols via factor analysis of aerosol mass spectrometry: a review, Anal. Bioanal. Chem., 401, 3045–3067, doi:10.1007/s00216-011-5355-y, 2011.

Table 1. Limits of Detection (in µg m^{-3}) and relative uncertainties (in %) for each species used in the second PMF analysis.

	HOA	BBOA	OOA	NO_3	SO_4	NH_4	Cl	K	BC_{wb}	BC_{ff}
LoD (µg m^{-3})	0.1	0.1	0.1	0.12	0.28	0.51	0.1	0.02	0.1	0.1
u (%)	30	30	30	15	15	15	20	50	40	40

Title Page
Abstract Introduction
Conclusions References
Tables Figures
◀ ▶
Back Close
Full Screen / Esc
Printer-friendly Version
Interactive Discussion

Table 2. Bootstrap mapping of the 4-factor solution from the global PM_1 source apportionment analysis.

% of bootstrap mapping	Base SV-SA	Base Wood burning	Base LV-SA	Base Traffic
Boot SV-SA	100	0	0	0
Boot Wood burning	0	100	0	0
Boot LV-SA	0	0	100	0
Boot Traffic	0	0	0	100

Title Page
Abstract | Introduction
Conclusions | References
Tables | Figures
◀| |▶
◀ ▶
Back | Close
Full Screen / Esc
Printer-friendly Version
Interactive Discussion

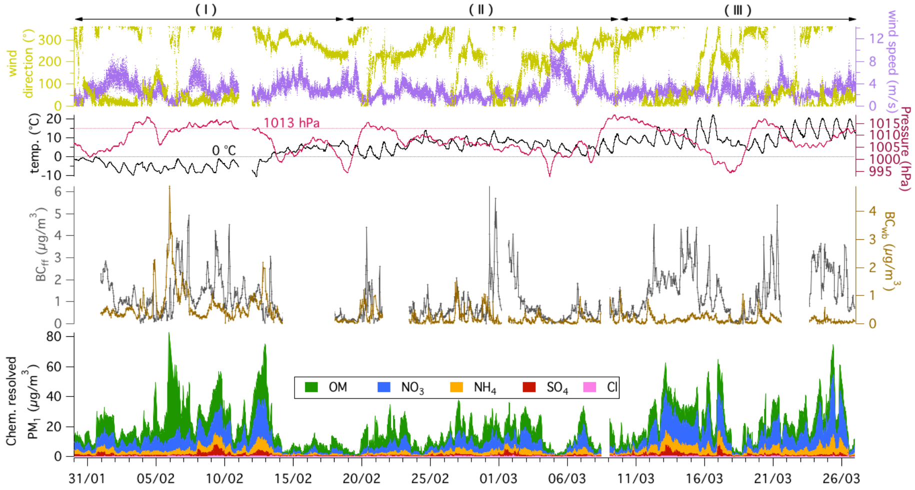

Figure 1. Meteorological parameters (ambient temperature, pressure, wind speed and direction); fossil fuel and wood burning fraction of black carbon measured by an Aethalometer; and Aerosol mass concentration of organics, nitrate, sulfate, ammonium and chloride measured by ACSM (note different scales).

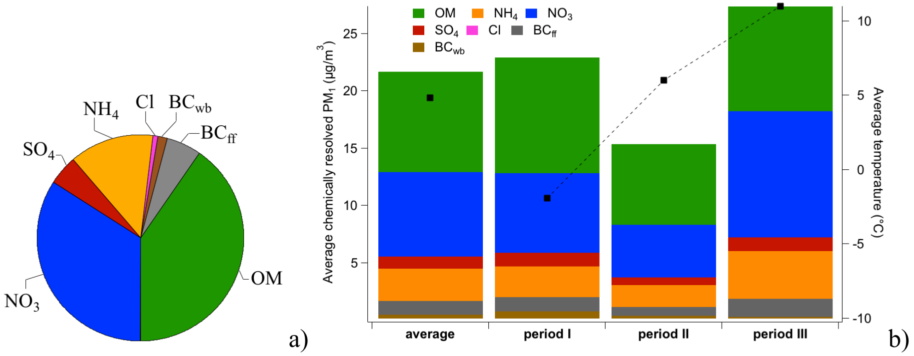

Figure 2. (a) Mean PM$_1$ chemical composition over the 2012 late winter period (average PM$_1$ = 21.7 µg m^{-3}) **(b)** Average PM$_1$ chemical composition (in µg m^{-3}) and ambient temperature over several periods.

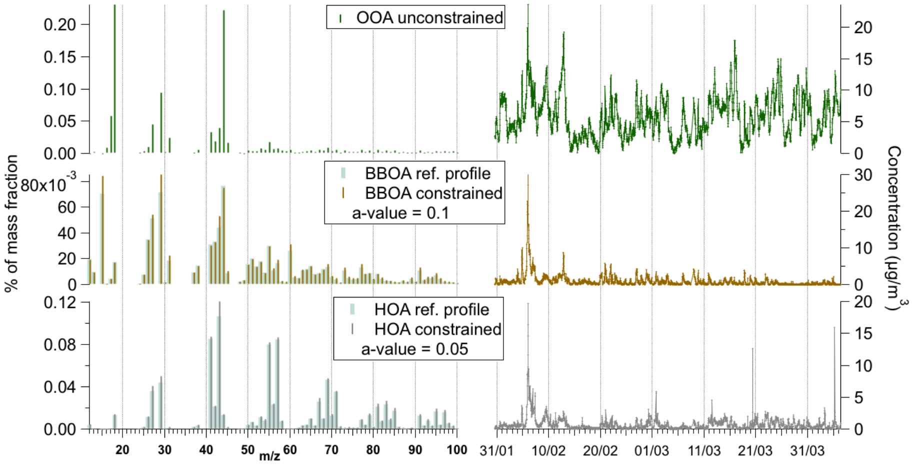

Figure 3. Factor profiles and timeseries of the 3-factor solution from the OA constrained PMF analysis.

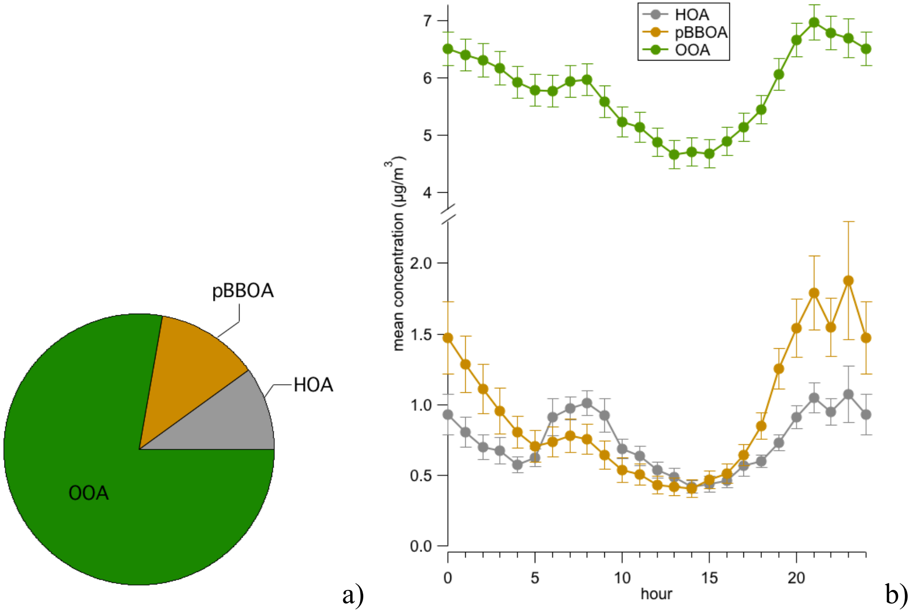

Figure 4. (a) Mean contribution to OM (in %) of the three organic factors **(b)** diurnal mean concentrations of the three organic factors.

Title Page
Abstract
Introduction
Conclusions
References
Tables
Figures
◀|
|▶
◀
▶
Back
Close
Full Screen / Esc
Printer-friendly Version
Interactive Discussion

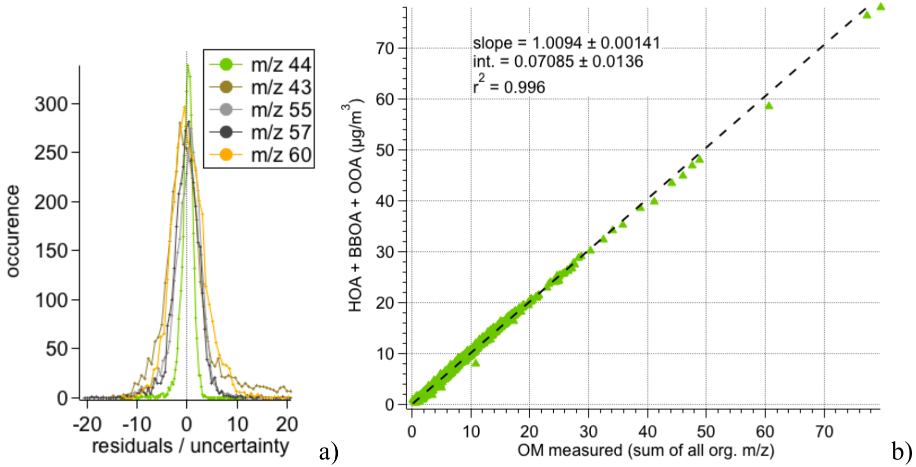

Figure 5. (a) Residuals distributions of m/z 44, 43, 55, 57 and 60 **(b)** Scatter plot of measured OM (sum of all m/z, row-wise) and calculated OM (sum of HOA + BBOA + OOA).

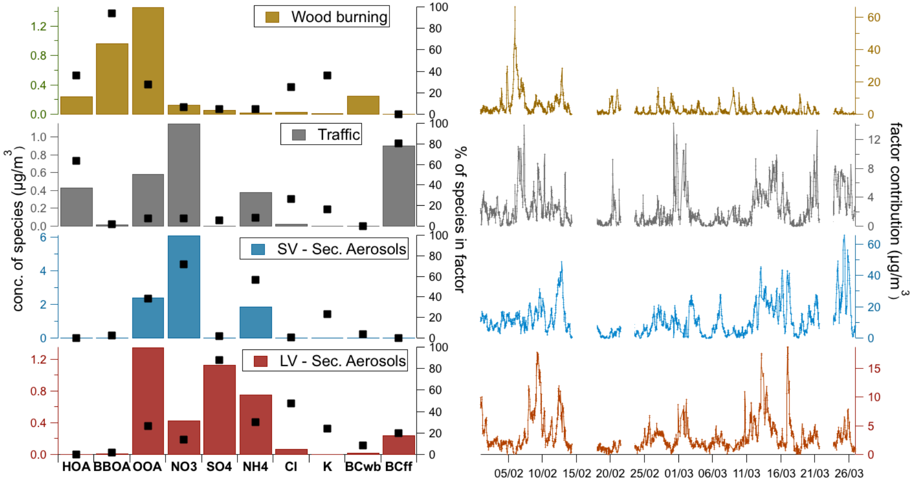

Figure 6. Factor profiles and timeseries for the 4-factor solution of the global PM_1 source apportionment analysis. Note the different scales.

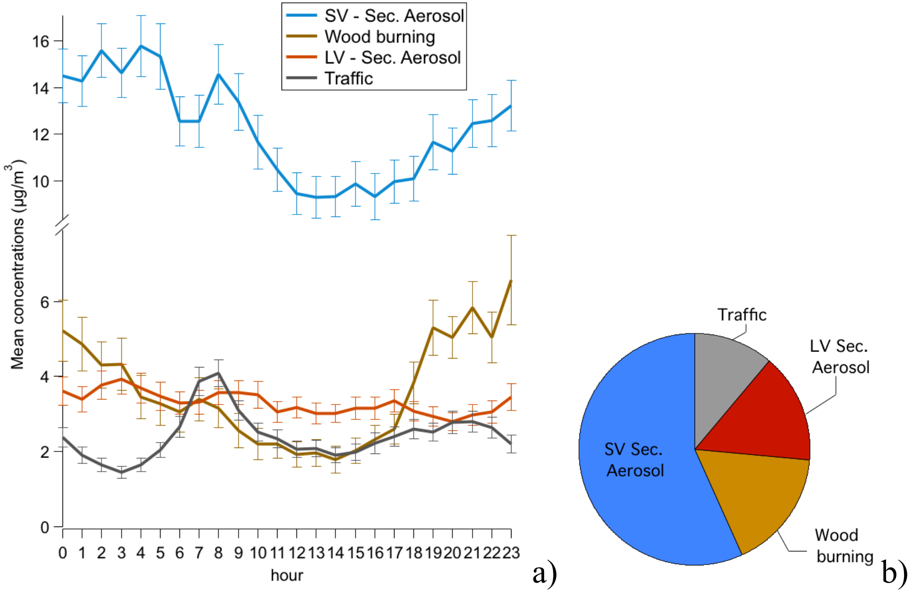

Figure 7. (a) Diurnal mean concentrations of the four factors **(b)** Mean contribution to PM_1 (in %) of the four factors.

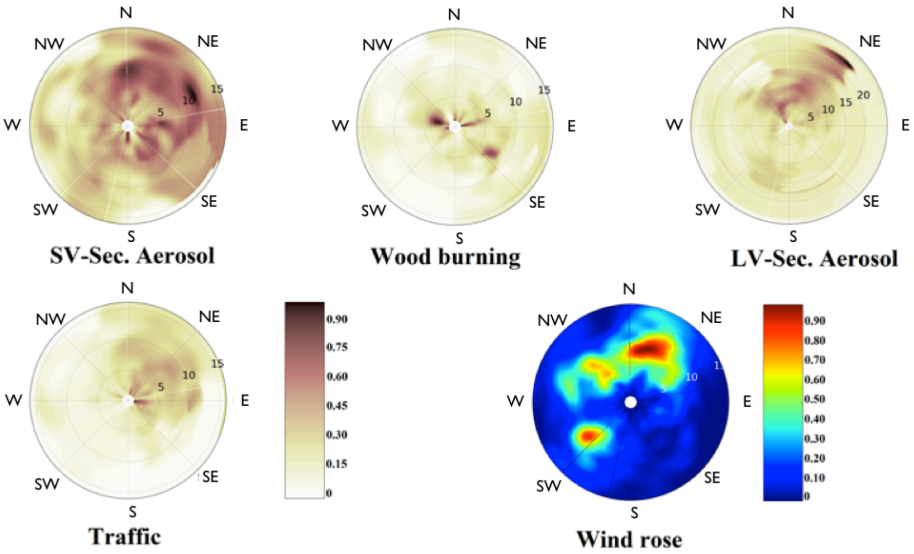

SV-Sec. Aerosol

Wood burning

LV-Sec. Aerosol

Traffic

Wind rose

Figure 8. Non-parametric Wind Regression normalized concentrations of the four factors, and the associated wind rose. Tangential and radial axes represent wind direction and speed (in km h^{-1}), respectively.

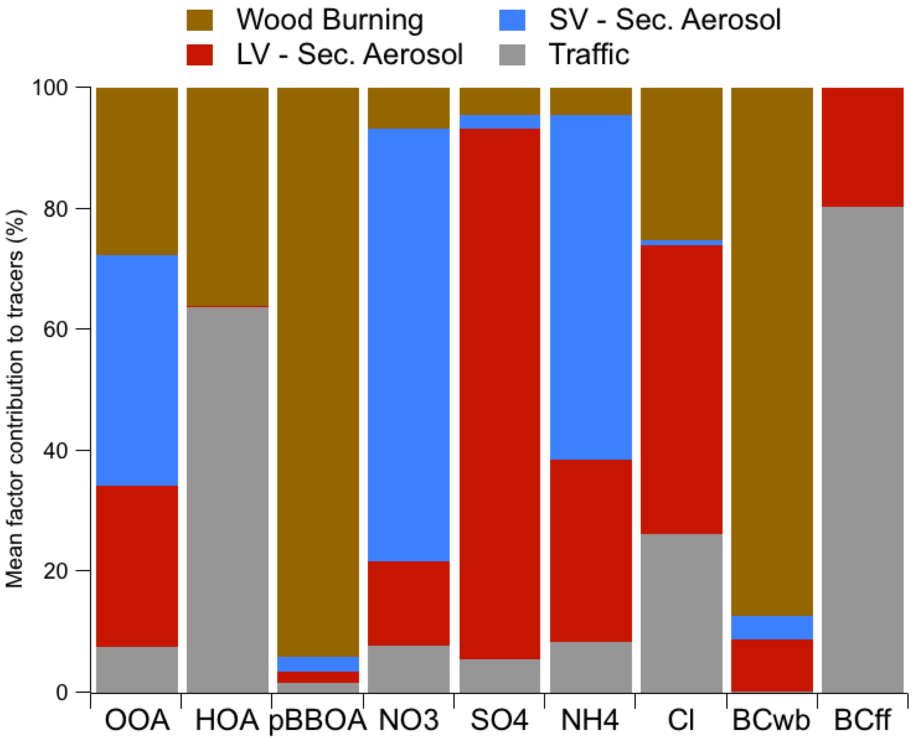

Figure 9. Mean factor contributions (in %) of the double PMF analysis to HOA, OOA, pBBOA, NO_3^-, SO_4^{2-}, NH_4^+, Cl^-, BC_{wb} and BC_{ff}.

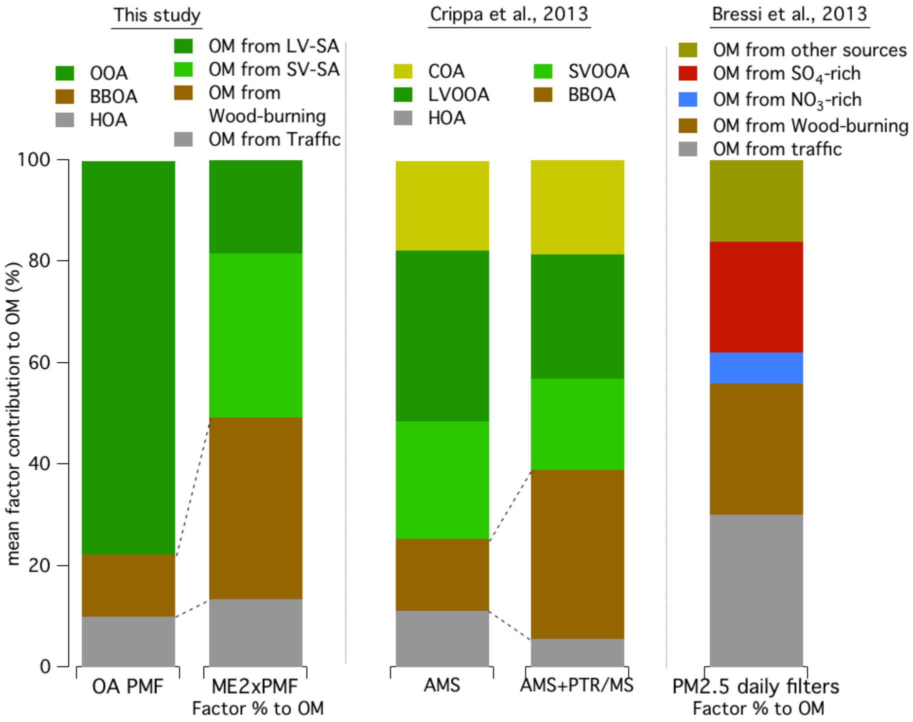

Figure 10. Comparison of source apportionment studies in Paris, France.